

MILITARY TECHNICAL COLLEGE
CAIRO - EGYPT7th INTERNATIONAL CONF. ON
AEROSPACE SCIENCES &
AVIATION TECHNOLOGY

AIRCRAFT LANDING PATH TRACKING USING THE ADAPTIVE FILTERING ALGORITHM

Elsayed A. Soleit* (Ph.D)

ABSTRACT

A proposal of an adaptive closed loop system for tracking the aircraft during the approach and landing maneuver is presented. The aircraft path is measured by the MLS integrated with the GPS systems. However, the measured path is combined with additional noise or interference signals that degrade the system performance. Then, the aircraft path should be estimated from noisy observations. In this paper, an adaptive filtering algorithm is applied rather than the Kalman filter to obtain an optimal estimate of the aircraft path to control the aircraft actuators. The adaptive filter coefficients are updated according to the least mean square adaptation algorithm. The performance of the proposed scheme is evaluated through the computer simulation during the lateral and longitudinal aircraft motion. It is concluded that the proposed scheme exhibits high convergence and tracking rates. Also, the proposed scheme produces small fluctuations during the aircraft tracking of an assigned reference path.

KEY WORDS

The adaptive filter, the adaptation algorithm, the adaptive control and tracking.

1- Introduction

The automatic path tracking of the aircraft during the approach and landing maneuver in the adverse weather conditions or at night flights is of great importance. This is due to the fact that the majority of the aircraft accidents occur during the approach and landing maneuver [1]. Moreover, the automatic path tracking can be applied in the smart weapons and self guided aircraft or missiles. The main features of the automatic path tracking system are based on an optimal update of the aircraft position such that a certain performance criterion or cost function is minimized. The wellknown performance criterion is the mean square or the least square of the deviation error between the reference and the measured path [1,2,3]. In this work, the aircraft current position is measured using the global positioning system (GPS) integrated with the standard microwave landing system (MLS). However, the measured data are severely corrupted with additional noise or interference which are not suitable to control the aircraft position actuators [1,2]. The Kalman filter is generally introduced to obtain a good

* Associate Professor, The Military Technical College

estimate of the aircraft position. However, the Kalman filter requires great computations and it is dependent on the aircraft model. [1-5]. In this paper a proposal of an adaptive path tracking scheme using the adaptive filtering algorithm is presented as depicted in Figure 1. The implementation of the adaptive filtering algorithm is easier and less complex than the Kalman one. The adaptive filter output is subtracted from an assigned reference path. The resulting error signal is applied to the aircraft control servos. The output of the control servos is adaptive controlled to update the aircraft control surfaces (elevator and rudder) such that the mean square of the error signal is minimized. The filter coefficients and the controller gains are updated according to the least mean square (LMS) adaptation algorithm [6].

This paper includes five sections. Section two explains the aircraft position coordinate systems while section three presents the adaptive path estimator. The simulation results are obtained in section four. Section five gives conclusions of the whole paper.

2- The Aircraft Position Coordinate System

The aircraft position in the space can be measured either in polar or rectangular coordinates with respect to a ground reference point (touch down point) using the GPS integrated with the MLS systems. Then, the aircraft position state vector is defined in rectangular coordinates as:

$$S_k = [x_k, y_k, z_k] \tag{1}$$

where x_k, y_k and z_k are the rectangular coordinates of the aircraft position. Also, the aircraft state vector can be written in the polar coordinates as:

$$S_k = [r_k, \gamma_k, \psi_k] \tag{2}$$

where r_k represents the aircraft range from a reference point (the touch down point) whose coordinates are represented by (x_0, y_0, z_0) . Also, γ_k represents the elevation angle or the glide path angle of the aircraft and ψ_k represents the aircraft azimuth with respect to the runway axis. Moreover, the polar coordinates can be expressed in terms of the rectangular coordinates as [1,2]:

$$r_k = \sqrt{(x_k - x_0)^2 + (y_k - y_0)^2 + (z_k - z_0)^2} \tag{3}$$

$$\sin(\gamma_k) = \frac{z_k - z_0}{r_k} \tag{4}$$

$$\sin(\psi_k) = \frac{y_k - y_0}{\sqrt{(x_k - x_0)^2 + (y_k - y_0)^2}} \tag{5}$$

The approach and landing path can be assigned a priori by a set of reference points or way points with respect to the touch down point.

It is assumed that the runway axis coincides with the X axis and the aircraft control in the longitudinal and the lateral motions are separable [1,2,7]. Consequently, the approach and landing path can be described in the space by its projections in the vertical and horizontal planes. The well known path model is expressed by a straight line sector with a constant glide path angle until a decision point and then, the aircraft completes the landing maneuver by flying along a curved path. The curved trajectory can be modeled by a variable glide path angle.

3- The Adaptive Path Estimator

The aircraft elevation and the azimuth angles can be measured using the GPS integrated with the MLS systems according to equations (1) to (5). However, the measured angles are highly corrupted with an additional noise which degrades the performance of the closed loop tracking system. Then, the measured azimuth and elevation angles should be enhanced using an adaptive path estimator to improve the performance of the adaptive tracking system. Hence, the function of the adaptive path estimator is to obtain good estimate of the measured elevation and azimuth angles. The outputs of the adaptive path estimator are used as feedback signals in the closed loop tracking system. The adaptive path estimator includes two adaptive filters; the elevation and the azimuth filters.

3.1 The elevation filter

The output of the elevation filter is defined by:

$$y_\gamma(k) = \alpha_k^T \beta_k \tag{6}$$

where α_k represents the coefficients vector of the elevation filter and β_k is known as the observation vector of the elevation angle. They are expressed respectively as:

$$\alpha_k^T = [a_0 \ a_1 \ \dots \ a_N] \tag{7}$$

and

$$\beta_k^T = [u_k \ u_{k-1} \ \dots \ u_{k-N}] \tag{8}$$

where u_k represents the measured observation of the elevation angle. It can be expressed as:

$$u_k = \gamma_k + n_k \tag{9}$$

where n_k represents the additive or the interference noise.

3.2 The azimuth filter

Also, the output of the azimuth filter can be expressed as:

$$\mathbf{y}_\psi(\mathbf{k}) = \rho_{\mathbf{k}}^T \boldsymbol{\eta}_{\mathbf{k}} \tag{10}$$

where $\rho_{\mathbf{k}}$ represents the coefficients vector of the azimuth filter and $\boldsymbol{\eta}_{\mathbf{k}}$ is known as the observation vector of the measured azimuth angle. They can be expressed respectively as:

$$\rho_{\mathbf{k}}^T = [\mathbf{c}_0 \mathbf{c}_1 \dots \dots \mathbf{c}_M] \tag{11}$$

and

$$\boldsymbol{\eta}_{\mathbf{k}}^T = [\mathbf{v}_{\mathbf{k}} \mathbf{v}_{\mathbf{k}-1} \dots \mathbf{v}_{\mathbf{k}-M}] \tag{12}$$

where $\mathbf{v}_{\mathbf{k}}$ denotes the measured azimuth angle and it can be written as:

$$\mathbf{v}_{\mathbf{k}} = \psi_{\mathbf{k}} + \mathbf{n}_{\mathbf{k}} \tag{13}$$

Furthermore, the error vector can be expressed in terms of the elevation and azimuth angles as:

$$\mathbf{E}_{\mathbf{k}} = [\varepsilon_\gamma \ \varepsilon_\psi] \tag{14}$$

where ε_γ and ε_ψ are the elevation and the azimuth deviation errors which are given by:

$$\varepsilon_\gamma = \gamma_r - \mathbf{y}_\gamma \tag{15}$$

$$\varepsilon_\psi = \psi_r - \mathbf{y}_\psi \tag{16}$$

where γ_r and ψ_r are defined as the desired glide path and azimuth angles of the reference path respectively.

3.3 The elevation and azimuth adaptation algorithms

The filter coefficients are updated according to the least mean square (LMS) adaptation algorithm [6] such that the mean square of the elevation and azimuth deviation errors are minimized. Hence, the LMS adaptation algorithm for the elevation and the azimuth coefficients can be derived as:

$$\alpha_{k+1} = \alpha_k + 2\mu \varepsilon_\gamma \beta_k^T \quad (17)$$

$$\rho_{k+1} = \rho_k + 2\mu \varepsilon_\psi \eta_k^T \quad (18)$$

where μ is a scalar quantity called the step size of the adaptation algorithm that controls the adaptation speed and the steady state adaptation noise.

3.4- The adaptive gain control

It is proposed in this work that the gain of the control servos is also updated according to the LMS adaptation algorithm such that the mean square of the elevation and azimuth errors is minimized. The adaptive output of the elevation control servo is defined as:

$$\mathbf{w}_\gamma = \mathbf{g}_\gamma(\mathbf{k}) \delta_e(\mathbf{k}) \quad (19)$$

where $\mathbf{g}_\gamma(\mathbf{k})$ represents the gain of the elevator controller and δ_e represents the output of the elevator control servo. Moreover, the adaptive output of the azimuth control servos is given by:

$$\mathbf{w}_\psi = \mathbf{g}_\psi(\mathbf{k}) \delta_r(\mathbf{k}) \quad (20)$$

where $\mathbf{g}_\psi(\mathbf{k})$ represents the gain of the rudder controller and δ_r represents the output of the rudder control servo. Hence, the gains of the elevator and rudder control servos are updated according to the LMS adaptation algorithm in [6] as:

$$\mathbf{g}_\gamma(\mathbf{k} + 1) = \mathbf{g}_\gamma(\mathbf{k}) + 2\mu \varepsilon_\gamma \delta_e(\mathbf{k}) \quad (21)$$

$$\mathbf{g}_\psi(\mathbf{k} + 1) = \mathbf{g}_\psi(\mathbf{k}) + 2\mu \varepsilon_\psi \delta_r(\mathbf{k}) \quad (22)$$

4- Simulation Results

The performance of the proposed adaptive tracking scheme depicted in Figure 1 is analyzed and evaluated through the computer simulation in the lateral and longitudinal motions. The elevator and the rudder servo transfer functions can be represented by first order systems as [7,8,9]:

$$\frac{\delta_e(z)}{\varepsilon_\gamma(z)} = \frac{10(1 - z^{-1})}{1 + 0.7z^{-1}} \quad (23)$$

$$\frac{\delta_r(z)}{\varepsilon_\psi(z)} = \frac{10(1-z^{-1})}{1+0.6z^{-1}} \quad (24)$$

Moreover, the aircraft longitudinal and lateral dynamics are represented using the short period approximation as [7,8,9]:

$$\frac{\theta(z)}{\delta_e(z)} = \frac{1}{1-0.96z^{-1}} \frac{-0.08644 - 0.025z^{-1} + 0.06389z^{-2}}{1-0.4966z^{-1} + 0.651z^{-2}} \quad (25)$$

$$\frac{\phi(z)}{\delta_r(z)} = \frac{1}{1-0.97z^{-1}} \frac{-0.09 - 0.036z^{-1} + 0.0545z^{-2}}{1-0.389z^{-1} + 0.6883z^{-2}} \quad (26)$$

The simulation results are demonstrated in the lateral and longitudinal motions as will be explained in the following sections.

4.1 The lateral motion

The azimuth angle observation is measured according to eq. (5), where the aircraft speed during the approach flight is assumed 200 m/sec. The initial aircraft azimuth angle is equivalent to $\psi = 0.1$ radian. The assigned reference azimuth angle with respect to the runway axis is equal to zero. Figure 2 illustrates the azimuth angle estimate versus the sampling time. Also, the system transient and the steady state lateral response is demonstrated by the system learning curve depicted in Figure 3. It is clear from figures 2 and 3 that the proposed scheme possesses high convergence rate and small residual mean square error (RMSE). The convergence time to the desired azimuth angle is equivalent to 1000 samples (sampling period = 10 msec) and the system provides $RMSE = 1.86 \times 10^{-6}$.

4.2 The longitudinal motion

The aircraft longitudinal motion during the landing maneuver is evaluated and measured by studying the behavior of the glide path estimate versus the sampling time (Sampling period = 10 msec) during the descent flight and flaring. The aircraft starts descent flight with an initial glide path angle equal to 0.12 radian and the aircraft landing speed is assumed 50 m/sec. Figure 4 demonstrates the glide path estimate versus the sampling time during the descent and flaring flight. It is apparent that the glide path estimate converges to the desired glide path angle after 1100 sampling time and the flaring (variable glide path angles) starts after 3000 sampling time. The glide path angle estimate converges to zero degree after 6000 samples at the assigned touch down point. Moreover, the decay of the aircraft height versus the sampling time is depicted in Figure 5. The transient and the steady state response of the adaptive tracking scheme is demonstrated using the system learning curve as shown in Figure 6. It is observed that the proposed scheme presents small convergence time and small fluctuations during the transient mode. Also, the proposed system provides a high tracking speed to follow the

variation of the desired glide path angle during the flaring maneuver. Furthermore, the system provides $RMSE = 1.6 \times 10^{-7}$ after convergence.

Moreover, the performance of the adaptive tracking loop for the longitudinal motion is evaluated and measured when the observed glide path angle is corrupted with an additional white gaussian noise at 1.2 dB signal to noise ratio (SNR). Figure 7 illustrates the noisy glide path angle without using the adaptive estimator at SNR = 1.2dB while the estimated glide path angle is demonstrated in Figure 8 using the adaptive estimator. The improvement in the output SNR is 6.6 dB.

5- Conclusions

It is concluded that the proposed adaptive tracking scheme to control the aircraft lateral and longitudinal motions exhibits a high convergence rate and small fluctuations. Also, the proposed scheme provides a high tracking speed to follow an assigned trajectory during the approach and landing maneuvers. The implementation of the path estimator using the adaptive filtering algorithm significantly improves the system performance and greatly reduces the computation complexity. Moreover, the real-time implementation of the proposed scheme can be carried out at a high sampling rate using the available aviation digital signal processors. Moreover, the proposal of updating the controller gain using the adaptation algorithm greatly improves the performance and stability of the adaptive tracking scheme.

Reference

- [1] Abo Elsoud M. S., Soleit E. A. and Osman M. S. "Automatic Landing System Using Kalman Estimator" The Second International Conference Engineering Research, Vol. 1, pp. 279-286, Suez Canal University, Port said, Egypt, Dec. 1995.
- [2] Halyo N, "Flight Tests OF The Digital Integrated Automatic Landing System(DIALS)"NASA, Scientific and Technical Information Branch, Langley, USA, 1984
- [3] Wang T.C and Varshney P. K "A Tracking Algorithm For Maneuvering Targets", IEEE TA On Aerospace and Electronic System, Vol-29, No. 3, July 1993.
- [4] Parkinson, B. W and Fitzgibbon, K. T", Aircraft Automatic Landing System using GPS", The Journal of Navigation, Vol. 42, No. 1, PP. 47-59, Stanford University, USA, Jan.1989.
- [5] Anderle H. T. , Schlabig, R. J. and Kulazycki J. S. "A Kalman Filter Application For Position Estimation of Airborne Relay Vehicle In The Precision Location Strike System", IEEE, National Aerospace Electronics, pp. 336-342, Ohio, USA, 1983.
- [6] Widrow B. and Stearn S. "Adaptive Signal Processing, New York, 1985
- [7] Robert C. N., "Flight Stability and Automatic Control", McGraw-Hill Book Company, New York, 1990.
- [8] Richard J. V., "Digital Control a State Space Approach", McGrew- Hill, INC, New York, 1995.
- [9] Boussalis and Others "Experimental Study in Adaptive Tracking Control", IEEE TA On Aerospace and Electronic Systems Vol-29, No. 4, Oct. 93.

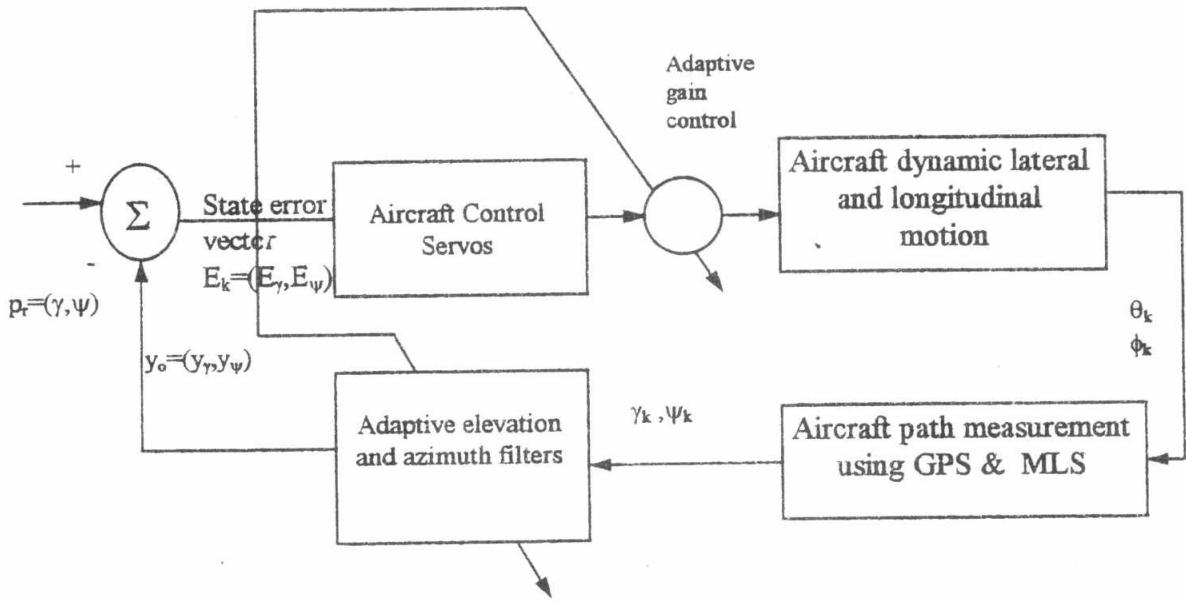


Fig. 1 The adaptive tracking scheme

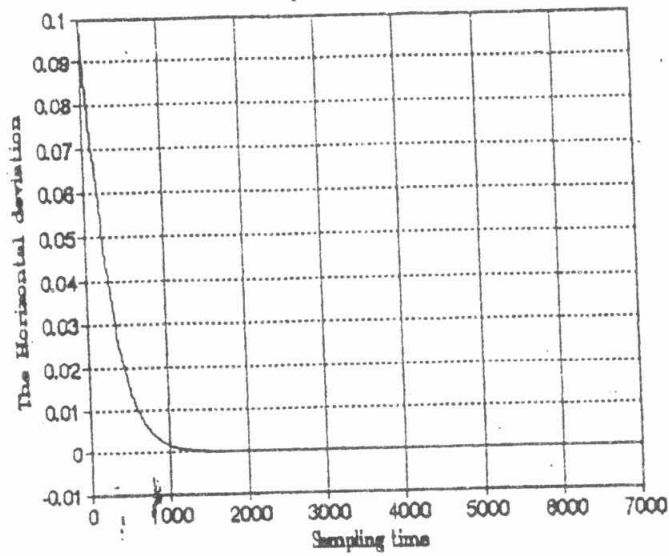


Fig. 2 The azimuth angle estimate ($N=5$, $\mu=0.011$, $RMSE=1.86 \times 10^{-6}$)

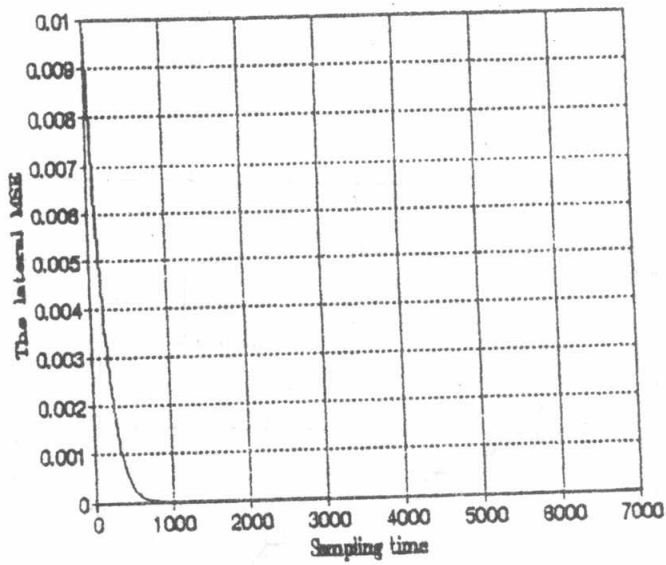


Fig. 3 The learning curve of the lateral tracking system
 (N=5, $\mu=0.011$, RMSE= 1.86×10^{-6})

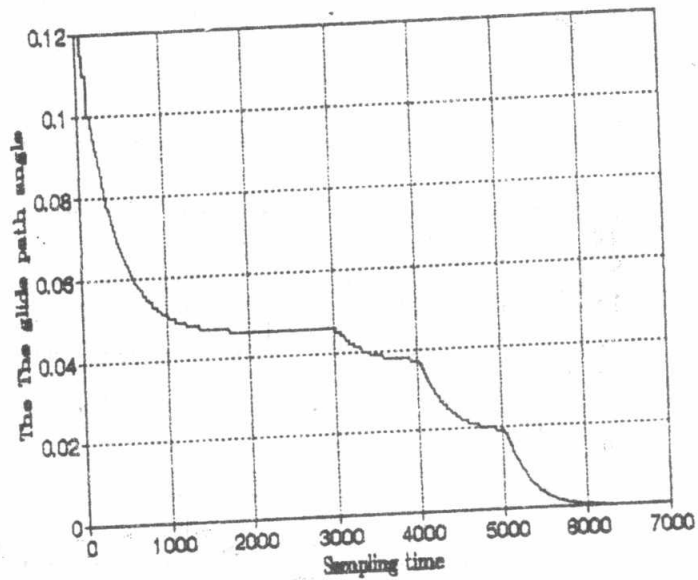


Fig. 4 The glide path estimate (N=4, $\mu=0.0125$, RMSE. = 1.6×10^{-7})

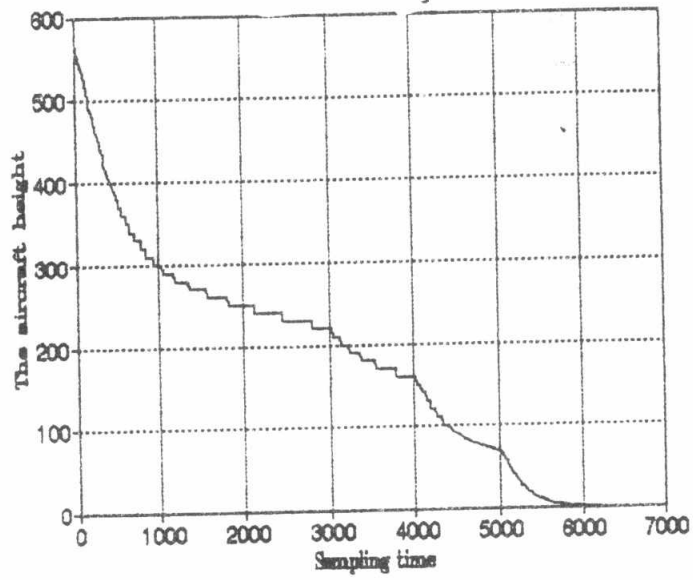


Fig. 5 The decay of the aircraft height during landing and flaring out

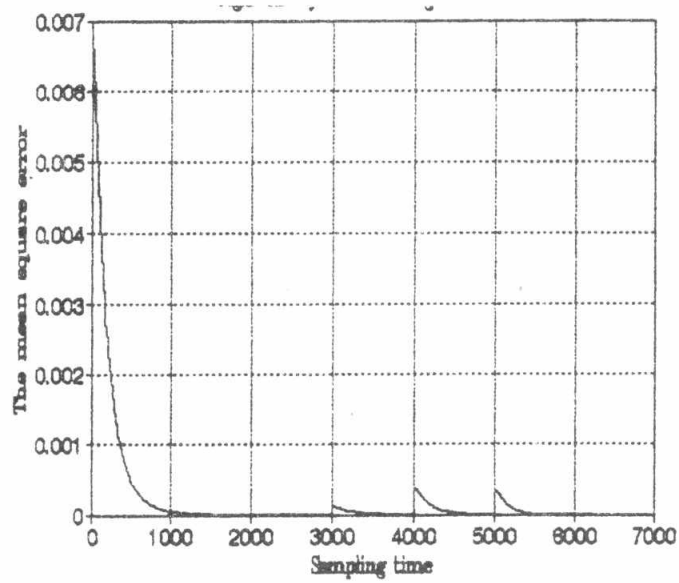


Fig. 6 The learning curve of the longitudinal tracking system

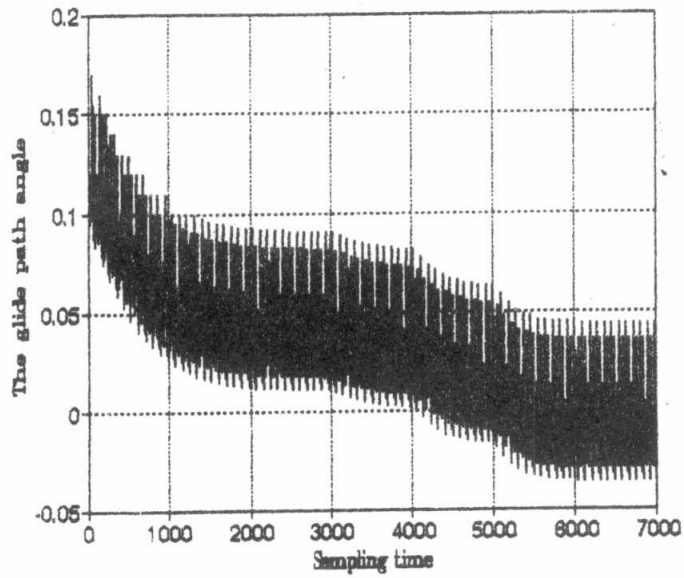


Fig. 7 The measured glide path angle without adaptive estimator at SNR=1.2 dB

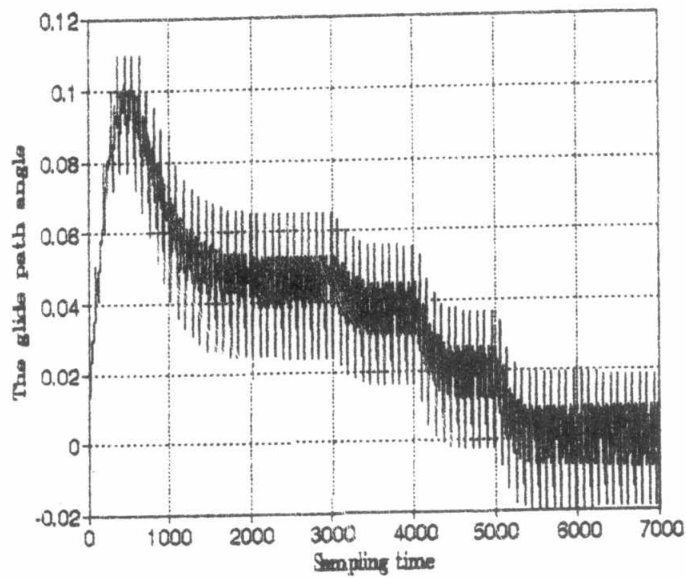


Fig. 8 The measured glide path angle with an adaptive estimator and 6.6 dB improvement